

Coherence of oscillations in matter and supernova neutrinos

Yago P. Porto-Silva*, Alexei Yu. Smirnov†

* Instituto de Física Gleb Wataghin - UNICAMP, 13083-859, Campinas, São Paulo, Brazil

* † Max-Planck-Institut für Kernphysik, 69117 Heidelberg, Germany

E-mail: *porto@mpi-hd.mpg.de, †smirnov@mpi-hd.mpg.de

Abstract

We study the propagation coherence for neutrino oscillations in media with different density profiles. For each profile, we find the dependence of the coherence length, L_{coh} , on neutrino energy and address the issue of correspondence of results in the distance and energy-momentum representations. The key new feature in matter is existence of energy ranges with enhanced coherence around the energies E_0 of "infinite coherence" at which $L_{coh} \rightarrow \infty$. In the configuration space, the infinite coherence corresponds to equality of the (effective) group velocities of the eigenstates. In constant density medium, there is a unique E_0 , which coincides with the MSW resonance energy of oscillations of mass states and is close to the MSW resonance energy of flavor states. In the case of massless neutrinos or negligible masses in a very dense medium the coherence persists continuously. In the adiabatic case, the infinite coherence is realized for periodic density change. Adiabaticity violation changes the shape factors of the wave packets (WPs) and leads to their spread. In a medium with sharp density changes (jumps), splitting of the eigenstates occurs at crossing of each jump. We study the increase of the coherence length in a single jump and periodic density jumps - castle-wall (CW) profiles. For the CW profile, there are several E_0 corresponding to parametric resonances. We outlined applications of the results for supernova neutrinos. In particular, we show that coherence between two shock wave fronts leads to observable oscillation effects, and our analysis suggests that the decoherence can be irrelevant for flavor transformations in the central parts of collapsing stars.

1 Introduction

Propagation coherence is the condition for realization of oscillations - the interference effects that lead to time - distance periodic variations of observables [1, 2, 3, 4, 5, 6, 7, 8, 9]. Correspondingly, decoherence means the disappearance of the interference and oscillatory pattern.

In the configuration space, the decoherence is produced by relative shift, and eventually, separation of the wave packets (WPs) that correspond to the eigenstates of propagation. The coherence length was defined as the distance at which the wave packets are shifted with respect to each other (separated) by the size of the wave packet σ_x , or equivalently, when the interference term in the probability is suppressed by a factor $1/e$. In the energy-momentum space, the decoherence is due to averaging of the oscillation phase over the energy interval of the energy uncertainty in a setup. It was checked that in vacuum and uniform matter, the two considerations are equivalent and lead to the same value of coherence length [10, 11, 12].

The loss of the propagation coherence does not lead to the loss of information and can be restored under certain conditions. In the configuration space, the restoration requires a long enough coherence time of detection. In the energy-momentum space it requires very good energy resolution. Irreversible loss of coherence occurs if neutrinos are treated as open quantum systems [13].

Mostly the coherence was studied for vacuum oscillation [1, 2, 3, 4, 5, 6, 7, 8, 9]. In matter with constant (or adiabatically changing) density it was considered in [11, 14, 15, 16, 12]. It was noticed that at certain energy (close to the MSW resonance energy), the difference of group velocities of the WPs vanishes in media with constant density and the coherence length becomes infinite [10, 11, 12]. If density varies with distance monotonously, then at a specific point, x_0 , near the MSW resonance, the difference of group velocities changes sign, and the shift that happened at $x < x_0$ can be undone at $x > x_0$, so that the packets overlap can be restored [11, 14, 12]. Decoherence affects resonant oscillations of solar and supernova neutrinos [15] and, in the case of supernova, decoherence happens before the resonance region. However, the effects of collective oscillations were not taken into account in [15]. In ref. [16], a formal solution for the neutrino equation of motion in general profile including non-adiabaticity was found. Based on it, the equivalence between x - and E -spaces was shown, at least for situations with $\sigma_E \ll E$. Limitations of the WP treatment were also discussed; in particular, as σ_E increases, negative energy components of the WPs become relevant. This can be important in situations with $\sigma_E \sim E$.

The coherence in the inner parts of supernova (SN) is of special interest [17]. The reason is that the wave packets of SN neutrinos are very short, $\sigma_E \sim E$, suggesting that decoherence can occur at smaller scales than the scales of possible collective oscillation phenomena [12, 18]. Furthermore, effectively, the problem is non-linear [19]. Therefore the question arises whether the loss of coherence destroys or not the collective phenomena [20].

In this paper, we consider coherence and decoherence in matter in detail. We revisit the case of the infinite coherence length in matter of constant density and give its physics interpretation. We show that in matter dominated regime, decoherence is determined by vacuum parameters. We comment on the fact that oscillations of massless neutrinos do not decohere. In the adiabatic case $L_{coh} \rightarrow \infty$ is possible if a density profile has periodic modulations. We then consider decoherence in the presence of adiabaticity violation. That includes decoherence in matter with single density jump which can be relevant for propagation through the shock wavefront in SN [12], and in the castle-wall profile [21, 22, 23, 24, 25]. The latter can give some idea about

the decoherence of collective oscillations in the inner parts of supernova [19]. The castle-wall profile is the simplest example because it admits analytical treatment and allows us to draw some conclusions about the relation between parametric resonances and coherence length.

Decoherence in the configuration (x -space) is equivalent to averaging of oscillation phase in energy or E -space for stationary situations [26]. Therefore, for each matter profile, we elaborate on the issue of equivalence of results in the x - and E -spaces. In particular, for the castle-wall profile, we show that the modification of shape factors in x -space due to the density jumps do not alter its Fourier transform and the initial energy spectrum of the WPs is preserved.

The paper is organized as follows: in section 2 we study the coherence length in vacuum and matter with constant and adiabatically varying density. We emphasize the existence of energies with infinite coherence length and give interpretation of $L_{coh} \rightarrow \infty$ in position and energy spaces. In section 3, we analyze coherence in the case of maximal adiabaticity violation. Section 4 presents the study of coherence in the castle-wall profile. Section 5 is devoted to the applications of our results to supernova neutrinos. In section 6 we present our conclusions.

2 Coherence in matter with constant and adiabatically changing density

In what follows for simplicity, we will consider the coherence in two neutrino system; the generalization to the case of three neutrinos is straightforward.

2.1 Coherence of oscillations in matter

In the energy-momentum space, the decoherence is related to averaging of the oscillation phase ϕ or the oscillatory (interference) term in probability P_{int} over the energy uncertainty, σ_E , of a set up¹. σ_E gives the width of the wave packet (WP), and in general, it is determined by the energy uncertainty at the production and detection, thus including a possibility of restoration of the coherence at the detection: $1/\sigma_E = 1/\sigma_E^{prod} + 1/\sigma_E^{det}$ [1, 2, 3, 4, 5, 6, 7, 16, 27, 12].

In the case of uniform medium (vacuum, constant density matter) the eigenstates and eigenvalues of the Hamiltonian of propagation H_{im} ($i = 1, 2$) are well defined [28, 10, 11, 14]. The difference of the eigenvalues, $\Delta H_m \equiv H_{2m} - H_{1m}$, determines the oscillation phase acquired along the distance L :

$$\phi_m = \Delta H_m L.$$

For a fixed L , variation of the phase with change of the neutrino energy E in the interval $E \pm \sigma_E$ equals

$$\Delta\phi_m = \left(2\sigma_E \frac{d\Delta H_m}{dE} + \frac{\sigma_E^3}{3} \frac{d^3\Delta H_m}{dE^3} + \dots \right) L. \quad (1)$$

¹There is subtle aspect related to averaging of ϕ and P_{int} which we will discuss later.

It increases linearly with L and we define the coherence length, L_{coh} , as the length at which the variation of oscillation phase becomes 2π :

$$|\Delta\phi_m(L_{coh}^m)| = 2\pi. \quad (2)$$

This condition means that averaging of the oscillatory dependence of the probability, which is a measure of interference, becomes substantial. Using the first term of the expansion (1) we obtain from the condition (2)

$$L_{coh}^m = \frac{\pi}{\sigma_E} \left| \frac{d\Delta H_m}{dE} \right|^{-1}. \quad (3)$$

At

$$\frac{d\Delta H_m(E)}{dE} = 0 \quad (4)$$

the coherence length becomes infinite [11, 14, 12]. The next terms in the expansions (1) shift the pole in (3) but do not eliminate it. The shift due to higher order terms is suppressed if $\sigma_E/E \ll 1$.

In vacuum

$$\Delta H = \frac{\Delta m^2}{2E},$$

where $\Delta m^2 \equiv m_2^2 - m_1^2$ is the mass square difference. Consequently, Eq. (3) gives

$$L_{coh} = \frac{\pi}{\sigma_E} \frac{2E^2}{\Delta m^2} = l_\nu \frac{E}{2\sigma_E}, \quad (5)$$

with $l_\nu = 4\pi E/\Delta m^2$ being the vacuum oscillation length. Notice that $L_{coh} \rightarrow \infty$ in the limits $E \rightarrow \infty$ or $\Delta m^2 \rightarrow 0$.

In matter with constant density [12], the difference of eigenvalues for a given matter potential is given by

$$\Delta H_m = \frac{\Delta m^2}{2E} \sqrt{\left(c_{2\theta} - \frac{2EV}{\Delta m^2}\right)^2 + s_{2\theta}^2}, \quad (6)$$

where θ is the vacuum mixing angle and $c_{2\theta} \equiv \cos 2\theta$ and $s_{2\theta} \equiv \sin 2\theta$. The derivative of (6) equals

$$\frac{d\Delta H_m}{dE} = \frac{\Delta m^2}{2E^2} \frac{\left(\frac{\Delta m^2}{2E} - V \cos 2\theta\right)}{\Delta H_m}. \quad (7)$$

Consequently, according to Eq. (3) the coherence length in matter equals

$$L_{coh}^m = \frac{L_{coh}}{l_m} \frac{2\pi}{\left|\frac{\Delta m^2}{2E} - V \cos 2\theta\right|} = L_{coh} \left(1 - c_{2\theta} \frac{2VE}{\Delta m^2}\right)^{-1} \sqrt{\left(c_{2\theta} - \frac{2VE}{\Delta m^2}\right)^2 + s_{2\theta}^2},$$

with L_{coh} given in (5) and $l_m = 2\pi/\Delta H_m$ being the oscillation length in matter.

Let us consider dependence of L_{coh}^m on energy. Its salient feature is existence of the pole at

$$E_0 = \frac{\Delta m^2}{2V \cos 2\theta}.$$

That is, the infinite coherence length $L_{coh}^m \rightarrow \infty$ is realized at finite energy E_0 , in contrast to the vacuum case. E_0 is related to the MSW resonance energy, $E_R = \Delta m^2 \cos 2\theta / 2V$, as

$$E_0 = \frac{E_R}{\cos^2 2\theta}. \quad (8)$$

Thus, $E_0 > E_R$ and it can be very close to E_R in case of small mixing. Since the width of the MSW resonance peak is $2 \tan 2\theta E_R \approx 2 \sin 2\theta E_R$, the pole is within the peak. Therefore, at E_0 , the transition probability is large.

In terms of E_0 or $x \equiv E/E_0$ the derivative (7) can be rewritten as

$$\frac{d\Delta H_m}{dE} = \frac{2\pi}{El_\nu} \frac{1-x}{\sqrt{(1-x)^2 + x^2 \tan^2 2\theta}}.$$

Consequently, the ratio of the coherence lengths in matter and in vacuum (3) becomes

$$\frac{L_{coh}^m}{L_{coh}} = \sqrt{1 + \frac{\tan^2 2\theta}{\left(1 - \frac{E_0}{E}\right)^2}}. \quad (9)$$

The ratio Eq. (9) as function of energy is shown in fig. 1. It has the universal form which depends on the vacuum mixing only. The value $L_{coh}^m/L_{coh} = 2$ corresponds to energies at both sides of the peak $E = E_0 (1 \pm \tan 2\theta/\sqrt{3})^{-1}$. Thus, for small θ the quantity $\Delta E = (2/\sqrt{3}) \tan 2\theta E_0$ characterizes the width of the peak.

At the MSW resonance, $E = E_R$, the ratio (9) equals

$$\frac{L_{coh}^m}{L_{coh}} = \frac{1}{\sin 2\theta}. \quad (10)$$

That is, the coherence length Eq. (10) is enhanced in comparison to the vacuum length. For example, if $\theta = \theta_{13} = 8.5^\circ$, we have $L_{coh}^m \approx 12L_{coh}$. In the resonance the oscillation length increases by the same amount: $l_m^R = l_\nu / \sin 2\theta$.

For $E \ll E_0$, *i.e.* in the vacuum dominance case, we have $L_{coh}^m \approx L_{coh}$. Interestingly, for $E \gg E_0$, (matter dominated region)

$$L_{coh}^m \approx \frac{L_{coh}}{\cos 2\theta}. \quad (11)$$

That is, L_{coh}^m is determined by the vacuum parameters, and for small θ it approaches the vacuum L_{coh} again. This has important implications for supernova neutrinos.

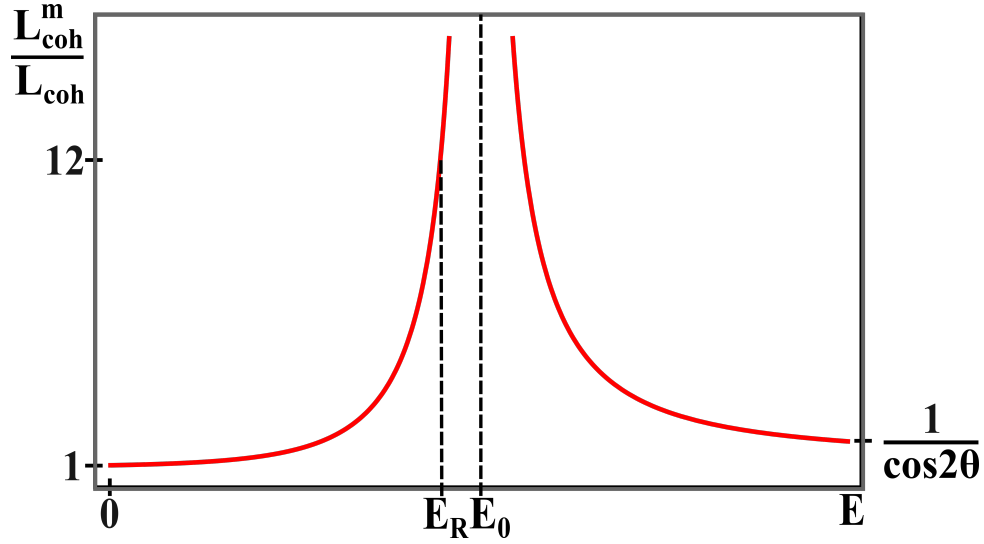


Figure 1: Dependence of the ratio L_{coh}^m/L_{coh} (9) on energy for $\theta = \theta_{13} = 8.5^\circ$. The ratio diverges at E_0 , and E_R is the MSW resonance energy.

The depth of oscillations in matter given by

$$\sin^2 2\theta_m = \frac{\sin^2 2\theta}{\left(\cos 2\theta - \frac{2EV}{\Delta m^2}\right)^2 + \sin^2 2\theta} \quad (12)$$

becomes at $E = E_0$

$$\sin^2 2\theta_m = \cos^2 \theta.$$

For $\theta = 8.5^\circ$ the depth is close to maximum: $\sin^2 2\theta_m \approx 0.98$. Therefore, in matter, strong flavor transitions can be preserved from decoherence over large distances L from the source to the detector.

2.2 Coherence in the configuration space

In the configuration space, the loss of propagation coherence is associated with relative shift and eventually separation of the wave packets of the eigenstates. The difference of group velocities of the eigenstates is given by

$$\Delta v_m = -\frac{d\Delta H_m}{dE}. \quad (13)$$

Then spatial separation (relative shift) x_{shift} of the packets after propagating a distance L equals

$$x_{shift}(L) = \int_0^L \Delta v_m dx = -\int_0^L \frac{d\Delta H_m}{dE} dx.$$

The coherence length L_{coh}^m can be defined as the distance at which the separation equals the spatial size of the packets σ_x : $|x_{shift}(L_{coh}^m)| \approx \sigma_x$. At this point, the overlap of the packets becomes small. In the case of constant density this condition gives

$$L_{coh}^m = \sigma_x \left| \frac{d\Delta H_m}{dE} \right|^{-1}. \quad (14)$$

Since $\sigma_x = 2\pi/(2\sigma_E)$ (recall that $\sigma_E \approx \sigma_p$ is the half-width), the expression (14) coincides with expression for the length in the energy representation (3). This shows the equivalence of the results in the configuration and the energy-momentum spaces.

According to Eq. (13) at $E = E_0$ the eigenstates in matter have equal group velocities and therefore do not separate. As a result, coherence is maintained during infinite time: $L_{coh}^m \rightarrow \infty$. Thus, in the configuration space the condition for infinite coherence is

$$v_1 = v_2. \quad (15)$$

The infinite coherence energy E_0 coincides with the resonance energy of oscillations of the mass eigenstates in matter $\nu_1 \leftrightarrow \nu_2$ [14]. This is not accidental. The origin of the energy dependence of phase, the difference of group velocities and therefore decoherence is the mass states. The resonance means that at E_0 the mass states ν_1 and ν_2 are maximally mixed in the eigenstates ν_i^m . That is, ν_1^m and ν_2^m both contain equal admixtures of ν_i . Consequently, the group velocities of ν_1^m and ν_2^m should be equal. In other words, in a given flavor state the components ν_1 and ν_2 oscillate with maximal depth $\nu_1 \rightarrow \nu_2 \rightarrow \nu_1 \rightarrow \nu_2$, which compensate separation.

The derivative of the oscillation length in matter equals

$$\frac{dl_m}{dE} = -\frac{2\pi}{(\Delta H_m)^2} \frac{d\Delta H_m}{dE}.$$

Therefore the condition of infinite coherence (4) coincides with the extremum of oscillation length. For a given potential V , $l_m^{max} = 2\pi/(V \sin 2\theta)$, which is larger than the length in the MSW resonance: $l_m^R = 2\pi/(V \tan 2\theta)$, and the difference is substantial for large vacuum mixing.

Notice that decoherence is related to uncertainty in energy on a certain interval of energy. Therefore infinite coherence energy should refer to the average energy in a wave packet.

Notice that the equivalence of results in two representations originates from the fact that the same quantity $d\Delta H_m/dE$ determines the change of the oscillation phase with energy (in $E - p$ space) on the one hand side, and the difference of the group velocities (in x -space) on the other hand.

2.3 Correlation of the phase difference and delay

The separation between the WP of eigenstates, $t \approx \Delta v X$, is proportional to their phase difference (oscillation phase), $\phi = \Delta H_m X$:

$$t = g(E, V)\phi, \quad (16)$$

where according to (7)

$$g(E, V) = \frac{\Delta v}{\Delta H_m} = \frac{1}{\Delta H_m} 2E^2 = \frac{1}{E} \frac{1 - \frac{2VEc_{2\theta}}{\Delta m^2}}{\left(c_{2\theta} - \frac{2VE}{\Delta m^2}\right)^2 + s_{2\theta}^2}.$$

In terms of infinite coherence energy, E_0 , it can be rewritten as

$$g(E, V) = \frac{2Vc_{2\theta}}{\Delta m^2} \frac{\frac{E_0}{E} - 1}{\left(c_{2\theta} - \frac{E}{E_0 c_{2\theta}}\right)^2 + s_{2\theta}^2}.$$

For $E \ll E_0$ (vacuum case)

$$g(E, V) = \frac{1}{E}.$$

At $E = E_0$ (near the MSW resonance): $g(E, V) = 0$ - there is no loss of coherence, and the oscillation phase, being non-zero, is suppressed by mixing:

$$\phi = \frac{\Delta m^2 X}{2E_0} \tan 2\theta = \phi_{vac}(E_0) \tan 2\theta.$$

For $E \gg E_0$ (matter dominated case):

$$g(E, V) \approx -\frac{c_{2\theta} \Delta m^2}{2VE^2} = -\frac{E_0 c_{2\theta}^2}{E^2}.$$

Here also the relative separation is strongly suppressed, while oscillations proceed with large phase $\phi \approx VX$.

Notice also that the relative separation changes the sign at E_0 . Therefore in layers a and b with two different densities one may have opposite sign of a delay and also $t^a = -t^b$ (see below). The phases do not change the sign and are always positive.

2.4 Physics of $L_{coh}^m \rightarrow \infty$

Here we present an interpretation of the divergence of L_{coh}^m at certain energy E_0 . The transition probability is given by

$$P_{\alpha\beta}(\theta_m, \phi_m) = \frac{1}{2} \sin^2 2\theta_m (1 - \cos \phi_m).$$

It should be averaged over the energy interval $2\sigma_E$. The change of $\sin^2 2\theta_m$ with energy in the interval $E_0 \pm \sigma_E$ equals

$$\left| 2\sigma_E \frac{d}{dE} \sin^2 2\theta_m \right| = 2\sigma_E \frac{Vc_{2\theta}}{\Delta m^2} = \frac{\sigma_E}{E_0} \ll 1,$$

where we have taken into account that at E_0 the mixing parameters are $\sin^2 2\theta_m = \cos^2 \theta$ and $\cos^2 2\theta_m = \sin^2 \theta$. Therefore $\sin^2 2\theta_m$ can be put out of the averaging integral at $E \sim E_0$. Furthermore, to simplify consideration, instead of averaging over E we will average $P_{\alpha\beta}$ immediately over the phase ϕ_m in the interval $2\delta\phi_m$ determined by

$$2\delta\phi_m = \frac{d\phi_m}{dE} 2\sigma_E = \frac{d\Delta H_m}{dE} L 2\sigma_E. \quad (17)$$

The averaging of the oscillatory term yields

$$\frac{1}{2\delta\phi_m} \int_{\phi_m - \delta\phi_m}^{\phi_m + \delta\phi_m} d\phi'_m P_{\alpha\beta}(\phi'_m) = \frac{1}{2} \sin^2 2\theta_m(E_0) [1 - D(\delta\phi_m) \cos \phi_m],$$

where

$$D(\delta\phi_m) \equiv \frac{\sin \delta\phi_m}{\delta\phi_m}$$

is the decoherence factor which describes suppression of the interference term.

According to (17) for $E = E_0$ the variation of phase is $\delta\phi_m = 0$, and consequently, $D(\delta\phi_m) \rightarrow 1$. The averaging effect is small in the region around E_0 . Indeed, $D(\delta\phi_m)$ has a peak centered at $\delta\phi_m = 0$. The half-width at nearly half of maximum, $D(\delta\phi_m) = 0.5$ corresponds to

$$|\delta\phi_m| \approx 1.89. \quad (18)$$

Consequently, the half-width of the peak in the energy scale, Γ , is determined by the condition

$$|\delta\phi_m(E_0 + \Gamma)| = 2$$

(rounding (18) to 2). Using this value and expressions in (17) and (7), we find the relative half-width of the peak:

$$\frac{\Gamma}{E_0} = \frac{\tan 2\theta}{\sqrt{\pi^2 d^2 - 1}}, \quad (19)$$

where

$$d \equiv \frac{\sigma_E L}{E_0 l_\nu}.$$

Notice that (19) requires $d\pi > 1$, or explicitly $L > l_\nu E / (\pi\sigma_E) \approx L_{coh}$. For $d\pi \rightarrow 1$, the width $\Gamma \rightarrow \infty$, which means that coherence is well satisfied for all the energies. Moreover, the peak disappears (half a height does not exist).

For $\pi d \gg 1$ the Eq. (19) becomes

$$\frac{\Gamma}{E_0} = \frac{\tan 2\theta}{\pi d} = \tan 2\theta \frac{E_0 l_\nu}{\sigma_E \pi L}. \quad (20)$$

The larger L , as well as σ_E , the narrower the peak. Also, according to (20) the width of the peak increases with energy:

$$\frac{\Gamma}{E_0} \propto E_0^2.$$

2.5 Adiabatic evolution and infinite coherence

In the case of slow adiabatic density change [10, 11, 14], one can introduce the instantaneous eigenstates and eigenvalues $H_{im}(x)$ and their difference $\Delta H_m(x)$, which are well-defined quantities. The adiabatic oscillation phase is given by the integral

$$\phi_m^{ad}(L) = \int_0^L dx \Delta H_m(N_e(x)). \quad (21)$$

A change of the phase with the energy in the interval $2\sigma_E$ equals

$$\Delta\phi_m^{ad}(L) = 2\sigma_E \int_0^L dx \frac{d}{dE} \Delta H_m(x),$$

where we permuted the intergration over x and differentiation over E . Then the condition for decoherence is $\Delta\phi_m(L_{coh}^m) = 2\pi$, or explicitly,

$$\left| \int_0^{L_{coh}^m} dx \frac{d}{dE} \Delta H_m(x) \right| = \frac{\pi}{\sigma_E},$$

and $d\Delta H_m(x)/dE$ is given in (7).

In the configuration space the adiabatic evolution means that there are no transitions between the eigenstates. Therefore a propagation is described by two wave packets, which do not change shape factors as in the constant density case. Separation of the WP equals

$$\Delta x(L) = \int_0^L dx \frac{d}{dE} \Delta H_m(x), \quad (22)$$

and from (21), (22) we obtain

$$\frac{d\phi_m^{ad}}{dE} = \Delta x(L),$$

which is the basis of equivalence of results in the x - and E -representations. In particular, the infinite coherence condition, $d\phi_m^{ad}/dE = 0$, corresponds to zero separation.

Let us consider coherence for different density (potential) profiles. For monotonous change of the potential the infinite L_{coh}^m can not be realized. Indeed, for a given E the pole condition is satisfied for specific value of the potential $V_0(E) = V(E, x_0)$ in specific point x_0 . In the point $x = x_0 + \Delta x$, where $V(x_0 + \Delta x)$ is outside the L_{coh} -peak, significant enhancement of coherence is absent and $L_{coh}^m < \Delta x$.

Certain increase of the coherence length can be related to the fact that at V_0 the derivative $d\Delta H_m(x)/dE$ changes the sign which suppresses the integral over x . This corresponds to the change of sign of the difference of the group velocities at E_0 (V_0).

For a layer with a given length L the energy of zero separation (complete overlap) is realized (22) when

$$\int_0^{x_0} dx \frac{d}{dE} \Delta H_m(x) = - \int_{x_0}^L dx \frac{d}{dE} \Delta H_m(x), \quad (23)$$

and $x_0 = x_0(E)$.

The infinite coherence can be achieved in the potential with periodic modulations:

$$V(x) = \bar{V}(1 + h \sin 2\pi x/X). \quad (24)$$

For a large X , the adiabaticity condition is satisfied. Zero separation of WP, $\Delta x = 0$, is realized when the difference of group velocities has different signs in the first and the second parts of the period. So, there is a continuous "catch-up" effect.

According to (7) the energy E_0 of infinite coherence is obtained from the condition

$$\lim_{L \rightarrow \infty} \int_0^L dx \frac{\left(\frac{\Delta m^2}{2E} - V \cos 2\theta\right)}{\Delta H_m(x)} = 0. \quad (25)$$

Around the zero value of nominator, denominator changes much slower and it can be put out of integral at some average value of the potential. Then the condition (25) reduces to

$$\frac{\Delta m^2}{2E} L - \cos 2\theta \int_0^L dx V(x) = 0.$$

Performing explicit integration with the potential (24) we obtain

$$\frac{\Delta m^2}{2E_0} \approx \cos 2\theta \bar{V} + \frac{h X}{\pi L} \sin^2 \frac{\pi L}{X}. \quad (26)$$

In the limit $L \rightarrow \infty$ the last term on the RHS of (26) can be neglected and for E_0 we obtain the same expression (8) as in constant density case with the average potential \bar{V} .

In general, if V varies about some average value \bar{V} (even irregularly), there may be energy where $L_{coh}^m \rightarrow \infty$.

2.6 Coherence for massless neutrinos

The limit $L_{coh}^m \rightarrow \infty$ is realized for oscillations of massless neutrinos, as originally introduced by Wolfenstein [28]. Here the oscillation phase is independent of neutrino energy. Recall that the propagation decoherence is related to the energy dependence of level splitting ΔH_m and shows up as averaging over energy. Therefore the decoherence does not exist for oscillations of massless neutrinos driven by potentials.

3 Coherence and adiabaticity violation

Adiabaticity violation means transitions between the eigenstates of propagation $\nu_{1m} \leftrightarrow \nu_{2m}$ and therefore change of shape of the WPs. Here we will consider the cases of extreme adiabaticity violation when $dV/dx \rightarrow \infty$, which corresponds to density jumps at certain spatial points.

Extreme adiabaticity violation combined with shift and separation of the WPs leads to splits and catch up of the WPs [12]. We will first illustrate these effects considering a single density jump.

3.1 Coherence in the case of single density jump

Consider a two layers (a and b) profile with density jump at a border between them. The layers have matter potentials V_a and V_b and lengths L_a and L_b , so that the total length equals $L \equiv L_a + L_b$. Let $\theta_k = \theta_m(V_k)$ be the flavor mixing angle in layer k , ($k = a, b$).

Suppose in the beginning of layer a the state is

$$\nu(x=0, t) = c'_a f_1(t) \nu_1^a + s'_a f_2(t) \nu_2^a, \quad (27)$$

where we use abbreviations $c'_a \equiv \cos \theta_a$, $s'_a \equiv \sin \theta_a$ and $f_i(t)$ are the shape factors of the wave packets normalized as

$$\int dt |f_i(t)|^2 = 1.$$

Evolving to the border between the layers a and b the state (27) becomes

$$\nu(L_a, t) = c'_a f(t - t_1^a) e^{i2\phi_1^a} \nu_1^a + s'_a f(t - t_2^a) e^{i2\phi_2^a} \nu_2^a. \quad (28)$$

Here t_i^a are the times of propagation in the a -layer, $t_i^a = L_a/v_i^a$, v_i^a are group velocities, and ϕ_i^a are phases acquired by the eigenstates taken at the average energies in the packets. We assume that in the beginning ($t = 0$) the shape factors of ν_1^a and ν_2^a are equal.

Crossing the border between a and b each eigenstate ν_i^a splits into eigenstates ν_j^b of the layer b :

$$\nu_1^a = c_\Delta \nu_1^b + s_\Delta \nu_2^b, \quad \nu_2^a = c_\Delta \nu_2^b - s_\Delta \nu_1^b, \quad (29)$$

where $\Delta \equiv \theta_b - \theta_a$. Inserting (29) into (28) we obtain the state in the beginning of layer b . Then to the end of the layer b the state (28) evolves to

$$\begin{aligned} \nu(L, t) = & \left[c'_a c_\Delta f(t - t_1^a - t_1^b) e^{i2(\phi_1^a + \phi_1^b)} - s'_a s_\Delta f(t - t_2^a - t_1^b) e^{i2(\phi_2^a + \phi_1^b)} \right] \nu_1^b + \\ & \left[c'_a s_\Delta f(t - t_1^a - t_2^b) e^{i2(\phi_1^a + \phi_2^b)} + s'_a c_\Delta f(t - t_2^a - t_2^b) e^{i2(\phi_2^a + \phi_2^b)} \right] \nu_2^b. \end{aligned} \quad (30)$$

We put out the common phase factor $e^{i2(\phi_1^a + \phi_1^b)}$ and introduce the phase differences,

$$\phi^a \equiv \phi_2^a - \phi_1^a \quad \text{and} \quad \phi^b \equiv \phi_2^b - \phi_1^b. \quad (31)$$

Then we make the time shift as $t' = t - t_1^a - t_1^b$, which allows us to express results in terms of the relative time shifts of the eigenstates 1 and 2 in the layers a and b :

$$t^a \equiv t_2^a - t_1^a \quad \text{and} \quad t^b \equiv t_2^b - t_1^b. \quad (32)$$

Using these quantities and projecting (30) onto ν_e we obtain the amplitude of $\nu_e \rightarrow \nu_e$ transition over the two layer profile:

$$\begin{aligned} A_{ee} = & c_\Delta \left[c'_a c'_b f(t') e^{-i\phi} + s'_a s'_b f(t' - t^a - t^b) e^{i\phi} \right] \\ & + s_\Delta \left[c'_a s'_b f(t' - t^b) e^{-i\phi'} - s'_a c'_b f(t' - t^a) e^{i\phi'} \right]. \end{aligned} \quad (33)$$

In this expression we put out the factor $e^{i(\phi^a + \phi^b)}$ and introduce

$$\phi \equiv \phi^a + \phi^b \quad \text{and} \quad \phi' \equiv \phi^a - \phi^b. \quad (34)$$

3.2 Specific examples

Let us consider specific cases.

1. Suppose $|t^a| \gg \sigma_t$, that is, the separation of the WPs in the layer a is larger than the coherence time, which means that the WPs are completely separated and coherence is lost. Suppose also that $|t^b| \ll \sigma_t$, *i.e.* loss of coherence in the layer b is negligible, $|t^b| \approx 0$. Then taking into account that the shape factors $f(t')$ and $f(t - t^a)$ do not overlap we obtain from (33)

$$P_{ee} = \int dt |A_{ee}|^2 = \int dt |f(t')|^2 \left| c'_a c'_b c_\Delta + c'_a s'_b s_\Delta e^{i2\phi^b} \right|^2 + \int dt |f(t' - t^a)|^2 \left| s'_a s'_b c_\Delta e^{i2\phi^b} - s'_a c'_b s_\Delta \right|^2. \quad (35)$$

We assume that change of the oscillation phase $\phi^b(t)$ along the WP is negligible, so that the oscillatory factors can be put out of the integral and take into account that integrations of the moduli squared of the shape factors give 1 due to normalization. As a result, we obtain

$$P_{ee} = \left| c'_a c'_b c_\Delta + c'_a s'_b s_\Delta e^{i2\phi^b} \right|^2 + \left| s'_a s'_b c_\Delta e^{i2\phi^b} - s'_a c'_b s_\Delta \right|^2. \quad (36)$$

Computing the amplitudes in the energy space, we need to use the plane waves so that $f(t) = 1$, and the energy dependent phases $\phi^a(E)$ and $\phi^b(E)$. The probability is given by

$$P_{ee} = \int dEF(E) |A_{ee}|^2, \quad (37)$$

where $F(E)$ is the energy spectrum of neutrinos that corresponds to the WP in the E - p space $F(E) = |f(E)|^2$ and $f(E)$ is the Fourier transform of $f(t)$. The amplitude (33) can be written as

$$A_{ee} = e^{-i\phi(E)} A_1 + e^{i\phi'(E)} A_2, \quad (38)$$

with

$$A_1 = c'_a \left[c'_b c_\Delta + s'_b s_\Delta e^{i2\phi^b(E)} \right], \quad A_2 = s'_a \left[s'_b c_\Delta e^{i2\phi^b(E)} - c'_b s_\Delta \right]. \quad (39)$$

Here A_i are the oscillations amplitudes of the eigenstates of the layer a , ν_i^a , in the layer b , $\nu_i^a \rightarrow \nu_e$. Inserting (38) into (37) we have

$$P_{ee} = \int dEF(E) \left[|A_1|^2 + |A_2|^2 + 2|A_1 A_2| \cos 2(\phi^a + \chi) \right], \quad (40)$$

where $\chi \equiv \text{Arg}(A_1^* A_2)$ depends on the phase ϕ^b . To compare this with consideration in the x -space we assume that $\phi^a \gg 1$ (which corresponds to large delay in the layer a). In contrast, the phase ϕ^b is relatively small, $\phi^b \ll 1$. In this case we can put all the terms but those which depend on ϕ^a in (40) out of the integral taking them at average value of E in the spectrum. Then due to normalization $\int dEF(E) = 1$ the expression (40) becomes

$$P_{ee} = |\bar{A}_1|^2 + |\bar{A}_2|^2 + 2|\bar{A}_1 \bar{A}_2| \int dEF(E) \cos 2(\phi^a + \chi). \quad (41)$$

Here \bar{A}_i are the amplitudes at the average value of energy. The last term is suppressed as $1/\phi^a$ and negligible for $\phi^a \gg 1$. Thus, the result (41), with A_i in (39), coincides with that in the x -representation (36).

In the example considered above, the result does not depend on L_a , and $L_a \rightarrow \infty$ is possible. In a sense, one can consider this as the case of infinite coherence since oscillations can be observed at the arbitrary long distance from the source. Thus, density jump and splitting of eigenstates induce or restore the interference and therefore oscillations. Here suppression of propagation coherence is determined by properties of layer b . That is, the problem is reduced to a single layer with constant density. Depending on initial mixing and $\Delta\theta$, crossing the density jump can lead to even stronger interference than at the beginning of layer a .

The situation described above is realized, *e.g.*, for the solar and supernova neutrinos oscillating inside the Earth, where a is the vacuum between the star and the Earth, and b is the Earth. In the high energy part of solar neutrinos: $c_a^2 \ll s_a^2$.

2. Suppose the layer b has density at which velocities of eigenstates are equal so that coherence is maintained for arbitrary large L_b and $t^b = 0$. Furthermore, suppose in the layer a the wave packets are completely separated, $L_a \rightarrow \infty$ which means that dependence on ϕ^a disappears. Then according to (33),

$$A_{ee} = c'_a c'_b c_\Delta f(t) e^{i\phi} - s'_a c'_b s_\Delta f(t - t^a) e^{i\phi'} + c'_a s'_b s_\Delta f(t) e^{-i\phi'} + s'_a s'_b c_\Delta f(t - t^a) e^{i\phi}. \quad (42)$$

The interference of the overlapping parts (they have the same argument in f) equals

$$t : 2c_a'^2 c'_b s'_b s_\Delta c_\Delta \cos 2\phi^b(t), \quad (t - t^a) : -2s_a'^2 c'_b s'_b s_\Delta c_\Delta \cos 2\phi^b(t - t^a). \quad (43)$$

At a detector, both oscillation phases are equal to ϕ^b , and, the sum of interference terms (after integration over time) is

$$\cos 2\theta_a \sin 2\theta_b s_\Delta c_\Delta \cos 2\phi^b. \quad (44)$$

This can be compared to the depth of interference in the beginning of the layer a : $0.5 \sin^2 2\theta_a$.

Regions of parameters exist where the depth increases after propagation in the two-layer profile.

Apart from the restoration of the interference, there is another phenomenon which will be important for our further consideration, namely, change of the shape of the WP at crossing the border between the layers:

- Each packet ν_i^a becomes the two-component one with an overall size extended by the relative delay in the layer a , t^a .
- According to (42) the amplitudes of components of ν_1^b equal $(c'_a c_\Delta, -s'_a s_\Delta)$ for the earlier and the later ones correspondingly. The amplitudes in ν_2^b are $(c'_a s_\Delta, s'_a c_\Delta)$.

- The shape depends on the size of density jump. If, *e.g.*, the jump is small, $s_\Delta \sim s'_a \sim \epsilon \ll 1$, we find from the previous item the amplitudes for ν_1^b : $(1, \epsilon^2)$, and for ν_2^b : (ϵ, ϵ) . If $s_\Delta \approx c_\Delta$, the packets will have similar form with similar amplitudes ν_1^b : $(c'_a, -s'_a)$ and ν_2^b : (c'_a, s'_a) . If $s_\Delta = 1$, $c_\Delta = \epsilon$ we have ν_1^b : (ϵ, ϵ) and ν_2^b : $(1, \epsilon^2)$.

3. Consider the case $t^a = -t^b$, when separation in the layer b compensates separation in a . In spite of this compensation, and in contrast to the constant density or adiabatic cases, there is no complete overlap at the end of layer b due to split of the eigenstates. Only WP of A_{11} and A_{22} components will overlap completely, where subscripts indicate eigenstates in which a given final component propagated in layer a and b (*e.g.* A_{11} is the amplitude of WP $\nu_1^a \rightarrow \nu_1^b$). The component A_{12} will shift forward by t^a and A_{21} backward by t^a with respect to overlapping components, or vice versa, depending on the sign of t^a . If $|t^a| > \sigma_x$, only A_{11} and A_{22} interfere and the interference term equals

$$0.5 \sin 2\theta_a \sin 2\theta_b c_\Delta^2 \cos 2(\phi^a + \phi^b), \quad (45)$$

which again can be bigger than interference in the beginning of the layer a .

4. In the case $t^a \approx 0$, there is no separation and loss of coherence in the layer a . The components A_{11} and A_{21} as well as A_{22} and A_{12} will overlap, there is no split of eigenstates at the border $a \rightarrow b$.

There is no unambiguous way of introducing the coherence length in the presence of density jump in the profile. Recall that the equivalence in the E - and x -representations is established at the level of averaging of the oscillation phase and separation of the WP. In the case of a single jump, there are two different oscillation phases and two different delays due to splitting of eigenstates. The introduction of a single effective phase and effective delay is non-trivial. As we will see in sect. 4, this can be done for periodic structures with density jumps.

3.3 Wave packets in the x - and E -representations

Split of the eigenstates and delays of splitted components lead to substantial modifications of the shape factor of the total WPs, $\psi_i(x, t)$, in the x -space. At the same time, the Fourier transforms of $\psi_i(x, t)$ determine the neutrino energy spectrum. Let us show that despite substantial modifications of $\psi_i(x, t)$, the energy spectrum remains unchanged, as it should be [26].

Suppose $f(E)$ is the Fourier transform of $f(t)$, then in the E -representation the initial state (27) is

$$\nu(x=0, E) = f(E)(c'_a \nu_1^a + s'_a \nu_2^a).$$

The energy spectrum of this state equals

$$F(E) = |f(E)c'_a|^2 + |f(E)s'_a|^2 = |f(E)|^2. \quad (46)$$

Consider the simplest element of the profile which leads to modification of the shape factor: the layer a with constant density and density jump at the end (general case is just repetition

of this element). State (30), at the beginning of layer b ($t_i^b = 0$ and $\phi_i^b = 0$) in terms of $\psi_i(x = L_a, t)$ is

$$\nu(L_a, t) = \psi_1(L_a, t)\nu_1^b + \psi_2(L_a, t)\nu_2^b, \quad (47)$$

where the total WPs equal

$$\begin{aligned} \psi_1(L_a, t) &= [c'_a c_\Delta f(t) - s'_a s_\Delta f(t - t^a) e^{2i\phi^a}], \\ \psi_2(L_a, t) &= [c'_a s_\Delta f(t) + s'_a c_\Delta f(t - t^a) e^{2i\phi^a}]. \end{aligned} \quad (48)$$

Here we made time shift by t_1^a and put out common phase ϕ_1^a . In the beginning, ψ_i are the elementary WPs, $f(t)\nu_i^a$, as in (27), but along the propagation their widths increase and their forms change.

In E -space, the state just after crossing the density jump, $\nu(L_a)$, in Eq. (47), is:

$$\nu(L_a, E) = \psi_1(L_a, E)\nu_1^b + \psi_2(L_a, E)\nu_2^b, \quad (49)$$

The Fourier transform of $f(t - t^a)$ is $f(E)e^{iEt^a}$, so that

$$\begin{aligned} \psi_1(L_a, E) &= [c'_a c_\Delta - s'_a s_\Delta e^{-iEt^a + 2i\phi^a}] f(E), \\ \psi_2(L_a, E) &= [c'_a s_\Delta + s'_a c_\Delta e^{-iEt^a + 2i\phi^a}] f(E). \end{aligned}$$

Using these expressions, we find the energy spectrum

$$F(E) = |\psi_1(L_a, E)|^2 + |\psi_2(L_a, E)|^2 = |f(E)|^2,$$

which coincides with (46).

4 Coherence in the castle-wall profile

One can introduce the coherence length in the case of a periodic structure with a sharp density change. The castle-wall (CW) profile is multiple repetitions of the two layer structure considered sect. 3. This is an explicitly solvable example of the periodic profile, which can give an idea about effects in profiles with sine (or cosine) type of dependence on distance [21, 24, 25].

4.1 Parametric oscillations in the energy-momentum space

The oscillation probability after crossing n periods can be obtained from the probability for a single period computed above. Indeed, the amplitude A_{ee} (38),(39) can be written as

$$A_{ee} = R + iI_3,$$

where the real and imaginary parts of the amplitude equal respectively, see [24, 25],

$$R = c_a c_b - s_a s_b \cos(2\theta_a - 2\theta_b), \quad (50)$$

and

$$I_3 = -(s_a c_b \cos 2\theta_a + s_b c_a \cos 2\theta_b).$$

Then the probability is given by

$$P_{ee} = R^2 + I_3^2.$$

Similarly to A_{ee} one can find the amplitudes $A_{e\mu}$, $A_{\mu e}$ and $A_{\mu\mu}$ which compose the evolution matrix U_L over one period. The matrix allows to reconstruct the Hamiltonian integrated over the period: $iH_{CW}L = I - U_L$. Diagonalization of this Hamiltonian gives the eigenstates, *i.e.* mixing and difference of eigenvalues which allow to write the transition probability after passing n periods of size L , $P = |U(nL)_{\alpha\beta}|^2$, as

$$P(\nu_\alpha \rightarrow \nu_\beta, nL) = \left(1 - \frac{I_3^2}{1 - R^2}\right) \sin^2(n\xi). \quad (51)$$

Here ξ is the effective phase acquired over period:

$$\xi \equiv \arccos R.$$

The factor in front of sine gives the depth of the parametric oscillations. The depth is maximal at $I_3 = 0$, or explicitly

$$s_a c_b \cos 2\theta_a + c_a s_b \cos 2\theta_b = 0, \quad (52)$$

which is the condition of the parametric resonance. For arbitrary mixings the condition is satisfied for values of phases

$$\phi^a = \frac{\pi}{2} + k\pi \quad \text{and} \quad \phi^b = \frac{\pi}{2} + k'\pi.$$

In general, $I_3 = 0$ requires specific correlations between phases and mixings. The transition probability (51) reaches maximum, $P = 1$, when

$$n\xi = \frac{\pi}{2} + k\pi.$$

In what follows for illustration of the results we will use a castle-wall profile with $n = 5$ periods and the following parameters:

$$V_a = 5.3 \times 10^{-4} \text{ eV}^2, \quad L_a = 4 \text{ km}, \quad V_b = 2 \times 10^{-5} \text{ eV}^2, \quad L_b = 2 \text{ km}. \quad (53)$$

We take the vacuum oscillation parameters $\theta = 8.5^\circ$ and $\Delta m^2 = 2.5 \times 10^{-3} \text{ eV}^2$.

The transition probability of parametric oscillations Eq. (51), as function of energy, is shown in fig. 2. The probability reaches maximum at $E \sim 2.2$ (MSW resonance), 3.1 and 7.7 MeV, where condition (52) is met.

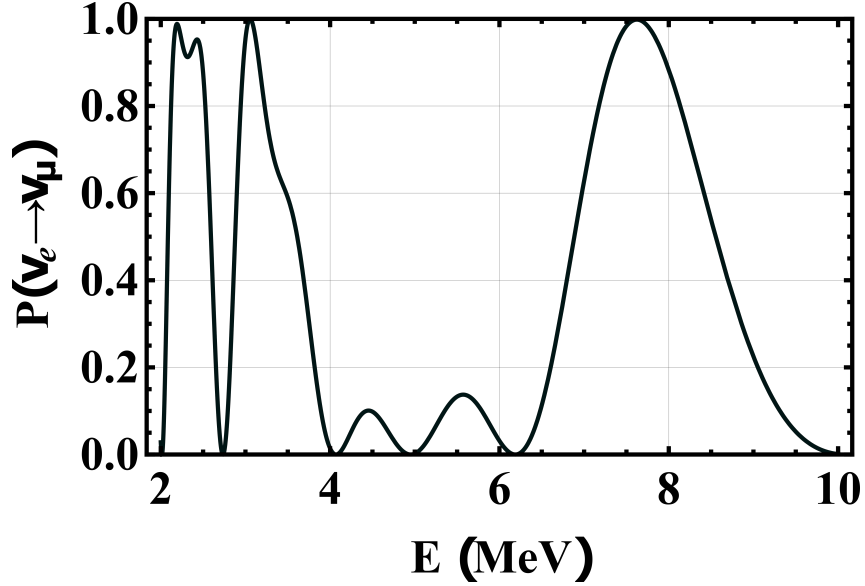


Figure 2: Transition probability of the $\nu_e \rightarrow \nu_\mu$ parametric oscillations as a function of neutrino energy for castle-wall profile with 5 periods. Parameters of the CW profile are given in Eq. (53). We used $\theta = 8.5^\circ$ and $\Delta m^2 = 2.5 \times 10^{-3} \text{ eV}^2$.

4.2 Coherence length in a castle-wall profile

In the energy representation we can repeat here the same procedure of determination of the coherence length as in the case of constant density. According to Eq. (51), the phase of parametric oscillations equals

$$\phi_n = n\xi = nL \frac{\xi}{L}.$$

Therefore the effective difference of eigenvalues equals

$$\Delta H_{cw} = \frac{\xi}{L}.$$

We introduce n_{coh} , the number of periods over which the coherence is maintained, so that $L_{coh} = n_{coh}L$. Using Eq. (3) for the coherence length we find

$$n_{coh} = \frac{\pi}{\sigma_E} \left| \frac{d\xi}{dE} \right|^{-1}.$$

According to (3) and (50)

$$\frac{d\xi}{dE} = -\frac{1}{\sqrt{1-R^2}} \frac{dR}{dE}, \quad (54)$$

and consequently,

$$n_{coh}(E) = \frac{\pi \sqrt{1-R^2}}{2\sigma_E \left| \frac{dR}{dE} \right|}. \quad (55)$$

The condition for infinite coherence length, $L_{coh} \propto n_{coh} \rightarrow \infty$, is

$$\left| \frac{d\xi}{dE} \right| = 0, \quad \text{or} \quad \frac{dR(E)}{dE} = 0, \quad (R \neq 1). \quad (56)$$

Since $R(E)$ is an oscillatory function of E , and therefore has several maxima and minima at certain energies E_0^i , the condition (56) is satisfied at these energies $E = E_0^i$.

As in the case of constant density, averaging of probability over the energy intervals σ_E leads to the appearance of the decoherence factors $D_i(E)$, (18), centered at energies E_0^i . Let us find the widths of the peaks of $D_i(E)$ for fixed length of trajectory nL . As in constant density case, instead of averaging over E we perform averaging over the effective phase in the interval which corresponds to $2\sigma_E$:

$$\delta\phi_n = 2\sigma_E n \frac{d\xi}{dE}. \quad (57)$$

The decoherence factor

$$D(\delta\phi_n(E)) = \frac{\sin \delta\phi_n}{\delta\phi_n}$$

has a width Γ determined by the condition in (19). Plugging $\delta\phi_n$ from (57) in the above equation we obtain

$$\left| \frac{d\xi(E_0^i + \Gamma)}{dE} \right| = \frac{1}{\sigma_E n}. \quad (58)$$

For narrow peaks, $\Gamma \ll E_0^i$, we can expand the left hand side of Eq. (58) around E_0^i ; and take into account that $d\xi(E_0^i)/dE = 0$. Then Eq. (58) reduces to

$$\left. \frac{d^2\xi(E)}{dE^2} \right|_{E=E_0^i} \times \Gamma = \frac{1}{\sigma_E n}. \quad (59)$$

Differentiating $d\xi/dE$ in (54) over E we have

$$\left. \frac{d^2\xi(E)}{dE^2} \right|_{E=E_0^i} = -\frac{1}{\sqrt{1 - R^2(E_0^i)}} \frac{d^2R(E_0^i)}{dE^2}. \quad (60)$$

Then insertion of this into (59) gives

$$\Gamma \approx \frac{\sqrt{1 - R^2(E_0^i)}}{\sigma_E n \left| \frac{d^2R(E_0^i)}{dE^2} \right|}.$$

In the limits $E_0^i \ll E_a, E_b$ and $E_0^i \gg E_a, E_b$, where E_a and E_b are the MSW resonance energies, we have $\theta_a \approx \theta_b$, and therefore

$$R \approx \cos(\phi^a + \phi^b).$$

Since $d\xi/dE \propto d(\phi^a + \phi^b)/dE = 0$ at $E = E_0^i$ the equation (60) becomes

$$\left. \frac{d^2\xi}{dE^2} \right|_{E=E_0} \approx \left. \frac{d^2(\phi^a + \phi^b)}{dE^2} \right|_{E=E_0},$$

and the width equals

$$\Gamma_i \approx \frac{1}{\sigma_E n \left. \frac{d^2(\phi^a + \phi^b)}{dE^2} \right|_{E=E_0^i}}.$$

The widths Γ^i are narrower at lower energies due to faster variations of the half-phases ϕ^a and ϕ^b . Similarly to the case of constant matter density, the ranges of weak averaging effect of transition probability are smaller at lower E_0^i .

4.3 Infinite coherence and parametric resonance

The energies of infinite coherence, E_0^i , are correlated to the energies of parametric resonances, determined by the condition $I_3 = 0$. This correlation is analogous to the one in Eq. (8) for constant density. To show this, we consider the expressions for dR/dE and I_3 in three different regions of energies. Starting with the explicit expression for dR/dE ,

$$\begin{aligned} \frac{dR}{dE} = & -s_a c_b \frac{d\phi^a}{dE} - c_a s_b \frac{d\phi^b}{dE} - c_a s_b \cos(2\theta_a - 2\theta_b) \frac{d\phi^a}{dE} \\ & - s_a c_b \cos(2\theta_a - 2\theta_b) \frac{d\phi^b}{dE} + s_a s_b \sin(2\theta_a - 2\theta_b) \frac{d(2\theta_a - 2\theta_b)}{dE}. \end{aligned} \quad (61)$$

We obtain the following

1. Far from the MSW resonances of both layers: $E \ll E_a, E_b$, where $\theta_a \approx \theta_b \approx \theta$, or $E \gg E_a, E_b$ where $\theta_a \approx \theta_b \approx \pi/2$. In both cases $\cos(2\theta_a - 2\theta_b) \approx 1$, and consequently, $R \approx \cos(\phi^a + \phi^b)$. Therefore

$$\frac{dR}{dE} = -\sin(\phi^a + \phi^b) \frac{d(\phi^a + \phi^b)}{dE}$$

On the other hand

$$I_3 \approx \sin(\phi^a + \phi^b) \cos 2\theta_a.$$

So that, the condition $I_3 \rightarrow 0$ requires $\sin(\phi^a + \phi^b) = 0$ and consequently, $\frac{dR}{dE} \rightarrow 0$, which implies $n_{coh} \rightarrow \infty$.

2. In the MSW resonances: when E coincides with one of the resonance energies *e.g.* $E \approx E_a$, and is far enough from the other one, E_b , then $\theta_a = \pi/4$, $\theta_b = \theta \approx 0$ (small mixing) or $\pi/2$ and $d\theta_b/dE = 0$. Because $E_a \sim E_{0a}$, we can take in (61) $d\phi^a/dE = 0$ which becomes

$$\frac{dR}{dE} = (-c_a s_b \pm s_a c_b \cos 2\theta_a) \frac{d\phi^b}{dE} \pm 2s_a s_b \sin 2\theta_a \frac{d\theta_a}{dE}. \quad (62)$$

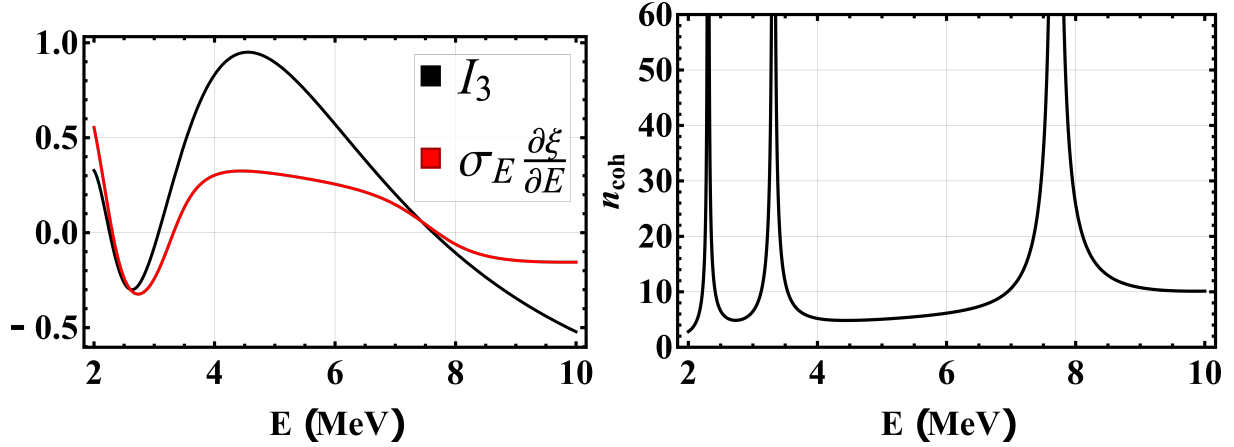


Figure 3: Left panel: I_3 and $\frac{d\xi}{dE}$ as function of neutrino energy. Right panel: Dependence of the n_{coh} in (55) on neutrino energy with $\sigma_E/E = 0.1$ MeV. The parameters of CW profile are the same as in fig. 2.

Here the upper sign is for $\theta_b \approx 0$ and the lower one $\theta_b \approx \pi/2$. We can rewrite (62) as

$$\frac{dR}{dE} = \pm I_3 \frac{d\phi^b}{dE} \pm 2s_a s_b \sin 2\theta_a \frac{d\theta_a}{dE}. \quad (63)$$

Assuming that $\sigma_E d\phi^b/dE \sim 1$ and $\sigma_E d\theta_a/dE \ll 1$, we find that the second term in (63) shifts the zero of dR/dE relative to the zero of I_3 . Nevertheless, E_0 is close to E_R , and the closer they are, the smaller $d\theta_a/dE$ is relative to $d\phi^b/dE$.

3. Between the MSW resonances: $E_a < E < E_b$ or $E_a > E > E_b$. If resonances are well separated, we have $|\theta_a - \theta_b| \approx \frac{\pi}{2}$ or $\cos(2\theta_a - 2\theta_b) \approx -1$. Therefore,

$$R \approx \cos(\phi^a - \phi^b),$$

and

$$\frac{dR}{dE} = -\sin(\phi^a - \phi^b) \frac{d(\phi^a - \phi^b)}{dE}.$$

On the other hand,

$$I_3 \approx -\sin(\phi^a - \phi^b) \cos 2\theta_1.$$

Consequently, $I_3 \rightarrow 0$ implies $dR/dE \rightarrow 0$, and $n_{coh} \rightarrow \infty$.

In the left panel of fig. 3 we show dR/dE and I_3 as functions of neutrino energy. I_3 is null at 2.25, 3.1 and 7.7 MeV, while the zeros of dR/dE , E_0^i are 2.3, 3.3 and 7.7 MeV. These coincidences show correlation of the parametric resonance and infinite coherence. The MSW resonance energies are $E_a = 2.25$ MeV and $E_b = 62.7$ MeV, outside the range of the plot.

On the right panel of fig. 3 we show dependence of n_{coh} on E for the CW profile with parameters (53) and $\sigma_E/E = 0.1$ MeV. n_{coh} diverges at the energies E_0^i . Notice that the shape of the peak is similar to MSW case in fig. 1. Thus, at the parametric resonance energies the averaging of oscillations is weak, and coherence is enhanced.

4.4 Coherence in castle-wall profile in the configuration space

In the x -representation, a picture of evolution in the CW profile is the following. Crossing every border between the layers a and b a given eigenstate of the layer a , ν_i^a , splits into two eigenstates of the layer b : $\nu_i^a \rightarrow \nu_1^b, \nu_2^b$. In turn, at the next border each eigenstate ν_j^b splits into eigenstates of a $\nu_j^b \rightarrow \nu_i^a$, etc. The amplitudes of the splits are determined by change of the mixing angles in matter (29).

As in subsection 4.1, 4.2 we consider that a flavor neutrino enters the layer a of the first CW period and a detector is placed at the border of b layer of the last period. After crossing n periods of the CW profile, each initially produced eigenstate ν_i^a ($i = 1, 2$) splits 2^{2n-1} times, and therefore at a detector there are 2^{2n} elementary components. The eigenstate ν_i^b ($i = 1, 2$), that arrives at a detector (last border), will be a composition of 2^{2n-1} such components. They will arrive at different moments and have different phases and amplitudes. We will assume that these elementary WPs are short enough and do not spread. Therefore the oscillation phases (phase differences) are the same along the elementary WPs. Each elementary WP has its "history" of propagation determined by type of eigenstate it showed up in each layer of the profile, e.g. $\nu_1^a \rightarrow \nu_2^b \rightarrow \nu_2^a \rightarrow \nu_1^b \rightarrow \nu_1^a \rightarrow \dots \rightarrow \nu_2^b$.

The elementary WPs compose the total WP of eigenstates ψ_i . Splits of eigenstates and delays lead to spread of total WP after crossing the CW profile. This spread affects the level of overlap and coherence. If a detector is sensitive to the flavor $\nu_f = c'_b \nu_1^b + s'_b \nu_2^b$, the detected signal is determined by

$$\int dt |c'_b \psi_1^b(t) + s'_b \psi_2^b(t)|^2. \quad (64)$$

where ψ_i^b are the total WP of the eigenstates ν_i^b in a layer b at a detector. The total WP, $\psi_j^b(t)$, can be found summing up all 2^{2n-1} elementary WPs at the detector.

A given elementary WP at the detector can be characterized by k_a and k_b - the numbers of a and b layers it propagates through as the second eigenstate, i.e. ν_2^m , $m = a, b$. Correspondingly, the numbers of layers it crossed as ν_1^m are $(n - k_a)$ and $(n - k_b)$. Using the same notation for phases, ϕ_i^a and ϕ_i^b ($i = 1, 2$), as in sect. 3 ($i = 1, 2$) we can write the total phase of a given elementary packet at a detector:

$$\phi(k_a, k_b) = \phi_1^a(n - k_a) + \phi_2^a k_a + \phi_1^b(n - k_b) + \phi_2^b k_b. \quad (65)$$

The phase difference between the elementary WPs characterized by k_a, k_b and k'_a, k'_b equals

$$\phi(k_a, k_b, k'_a, k'_b) = \phi^a(k_a - k'_a) + \phi^b(k_b - k'_b), \quad (66)$$

where we used definitions in (31).

Similarly one can find the relative time delays of arrival of the packets characterized by k_a, k_b and k'_a, k'_b at a detector using the definitions (32):

$$t(k_a, k_b, k'_a, k'_b) = t^a(k_a - k'_a) + t^b(k_b - k'_b). \quad (67)$$

As for the case of a single layer (16), there are the relations between the total delays (67) and total oscillation phases (66):

$$t(k_a - k'_a, k_b - k'_b) = \frac{d\phi(k_a - k'_a, k_b - k'_b)}{dE}, \quad (68)$$

and

$$t(k_a - k'_a, k_b - k'_b) = g(E, V)\phi(k_a - k'_a, k_b - k'_b). \quad (69)$$

Suppose, for definiteness, that t^a and t^b are positive, then maximal relative delay (separation) t^{max} corresponds to $|k_a - k'_a| = |k_b - k'_b| = n$:

$$t^{max} = n(t^a + t^b).$$

This is the time difference of arrival of the fastest and the slowest extreme elementary WP.

t^{max} separation determines the spread of whole WPs. The space between the fastest and the slowest WPs is filled in by non-extreme WPs. The extreme WPs are coherent if

$$n(t^a + t^b) \leq \sigma_x, \quad (70)$$

which gives the coherence number of periods (length)

$$n_{coh} \leq \frac{\sigma_x}{t^a + t^b}. \quad (71)$$

Under this condition, all other (intermediate) WP-components are also coherent (overlap). The condition (71) is sufficient but not necessary, since the coherence broken for extreme packets still can hold for intermediate packets.

Parameters k_a, k_b uniquely determine the phase and the delay of a given component. Number of components with a given k_a and k_b equals

$${}^n_{k_a}C \times {}^n_{k_b}C,$$

where n_pC is number of combinations of p elements from n elements. Apart from k_a and k_b the amplitudes of individual components are determined by the product of various mixing parameters: the initial and final flavor mixing, e.g. $c'_a c'_b$ for $\nu_e \rightarrow \nu_e$ channel and s_Δ, c_Δ determined by change of mixing at the borders between the layers Δ :

$$A(n, r, h) = (-1)^h c'_a c'_b s_\Delta^r c_\Delta^{2n-1-r}.$$

Factor s_Δ originates from each border at which the eigenstate number changes: $\nu_1^a \rightarrow \nu_2^b$, *etc.*, while c_Δ appears from the borders without change of eigenstate: $\nu_i^a \rightarrow \nu_i^b$. r is the number of borders where eigenstate changes; it is determined by the number of merging blocks: sequences of layers without change of eigenstate. h is given by the number of blocks with even number of sequential layers in which WP propagates as the second eigenstate.

For large number of periods there are many elementary packets with the same values of k_a, k_b, r, h . We call this number the multiplicity, $M(k_a, k_b, r, h)$. Therefore the total amplitude of all WPs with a given k_a, k_b equals

$$A(k_a, k_b) = \sum_{r,h} A(n, r, h) M(k_a, k_b, r, h). \quad (72)$$

As for the one period case, here the shape of the total WP depends on mixing and multiplicities.

For $k_a = k'_a, k_b = k'_b$ there is no shift but also the phase difference is zero. For $k_a - k'_a = 1, k_b - k'_b = 0$, the phase difference is ϕ^a , while for $k_a - k'_a = 0, k_b - k'_b = 1$ the phase difference is ϕ^b , *etc.* In general, one finds the components with phase differences varying from 0 to $n(\phi^a + \phi^b)$.

4.5 Resummation

We can obtain the compact expression for the total WPs summing up effects after each crossing of the CW period representing them as the interference of the two (total) WPs of ν_1^a and ν_2^a .

We consider first the summation in the basis of eigenstates of the layer a : $\nu^a = (\nu_1^a, \nu_2^a)$. Let $\psi^{k-1} = (\psi_1^{k-1}, \psi_2^{k-1})^T$ be the vector describing the state of system after crossing $k-1$ periods of the CW profile. ψ_i^{k-1} is result of resummation of the elementary WP of ν_i^a in the layer a in the beginning of k -period. Then after crossing of the k th period, the state becomes

$$\psi^k = U_L^a \psi^{k-1}, \quad (73)$$

where the evolution matrix over one period

$$U_L^a = U_\Delta D^b U_\Delta^\dagger D^a. \quad (74)$$

Here U_Δ is the matrix of the mixing change at crossing the border between a and b :

$$U_\Delta = U^{a\dagger} U^b = \begin{pmatrix} c_\Delta & s_\Delta \\ -s_\Delta & c_\Delta \end{pmatrix}, \quad (75)$$

and U^a, U^b are the flavor mixing matrices in the a and b layers. D^a is the evolution matrix in the layer a which can be written as

$$D^a = \begin{pmatrix} S(t_1^a) e^{i2\phi_1^a} & 0 \\ 0 & S(t_2^a) e^{i2\phi_2^a} \end{pmatrix} \quad (76)$$

Here $S(t_i^a)$ is the time-shift operator acting on the shape factor of the WP in such a way that

$$S(t_i^a)f_i(t) = f_i(t - t_i^a), \quad S(t_i^a)S(t_j^b) = S(t_j^b)S(t_i^a) = S(t_i^a + t_j^b) \quad (i, j = a, b).$$

We can also require that $S(t)^\dagger = S(-t)$, so that S is the unitary: $S(t)^\dagger S(t) = I$.

Similarly one can introduce the evolution matrix for the layer b . Inserting U_Δ and D_i^m ($m = a, b$) from (75) and (76) into (74) we obtain

$$U_L^a = \begin{pmatrix} c_\Delta^2 e^{-i\phi} + s_\Delta^2 S(t^b) e^{-i\phi'} & s_\Delta c_\Delta [S(t^b + t^a) e^{i\phi} - S(t^a) e^{i\phi'}] \\ s_\Delta c_\Delta [S(t^b) e^{-i\phi'} - e^{-i\phi}] & s_\Delta^2 S(t^a) e^{i\phi'} + c_\Delta^2 S(t^b + t^a) e^{i\phi} \end{pmatrix}, \quad (77)$$

where we subtracted the common phase factor $\exp\{i(\phi_2^b + \phi_2^a + \phi_1^b + \phi_1^a)\}$ and applied (31) and (34), as well as performed the time shift by $t_1^b + t_1^a$ and used (32). Using (77), we can recover results in sect. 3 for one period.

If all $S = 1$, we obtain the matrix which leads to the parametric oscillations as in [21, 23, 24].

The evolution matrix after n periods equals

$$U_{nL}^a = (U_L^a)^n. \quad (78)$$

According to (73) the total eigenstate is

$$\psi^n(t) = (U_L^a)^n f(t) \psi^0, \quad (79)$$

where $f(t)$ is the initial shape factor and ψ^0 are the admixtures of eigenstates ν_i^a in the initial moment of time. The components of ψ^n have the form

$$\psi^n = \sum_{k_a, k_b}^n A(k_a, k_b) f(t - k_a t^a - k_b t^b) e^{i(k_a \phi^a + k_b \phi^b)} \psi^0. \quad (80)$$

Notice from (80) that oscillations in energy are induced not only by interference between the total WPs of ψ_1^n and ψ_2^n but also by interference of components within amplitudes ψ_1^n and ψ_2^n with amplitudes (72).

The amplitude of the $\nu_e \rightarrow \nu_e$ transition equals

$$A_{ee}(t) = \nu_e^T (U_L^a)^n f(t) \nu_e, \quad \nu_e^T = (c_a, s_a). \quad (81)$$

This reproduces the amplitude for two layer case of sect. 4.1. Then the probability can be found as

$$P_{ee} = \int dt |\nu_e^T U_{nL}^a f(t) \nu_e|^2. \quad (82)$$

Various results can be obtained using the general form of amplitude and probability. One can consider evolution in the flavor basis, which corresponds to the derivation of the parametric oscillation probability in [21, 23, 24]. Now the evolution matrix equals

$$U_L^f = U^b D^b U_\Delta^\dagger D^a U^{a\dagger} = (U^b D^b U^{b\dagger})(U^a D^a U^{a\dagger}), \quad (83)$$

where in the last step the eigenstates of the layer b are projected onto the flavor basis. The matrices in the a eigenstate basis (74) and in the flavor basis (83) are related as

$$U_L^a = U^{a\dagger} U_L^f U^a. \quad (84)$$

The matrices after n layers:

$$(U_L^f)^n = U^a (U_L^a)^n U^{a\dagger}. \quad (85)$$

We can determine the effective Hamiltonian over one period using the evolution matrix over one period: $U_L = I - iHL$. Then diagonalizing the Hamiltonian gives the effective mixing and the eigenvalues, which, in turn, give the depth of the parametric oscillations and the phase. Clearly, such a Hamiltonian depends on mixing Δ and the phases of individual layers ϕ^a, ϕ^b .

4.6 Effective group velocities and infinite coherence in CW profile

In general, the condition of infinite coherence can be formulated as an equality of the effective group velocities of the wave packets:

$$v_1^{eff} = v_2^{eff} \quad (86)$$

or $\Delta v^{eff} = 0$. Determination v_i^{eff} depends on properties of the density profile and turns out to be non-trivial for the CW profile.

Recall that in the case of constant density v_i^{eff} are well defined, see (15) and related discussion. Since the shape factor does not change, the group velocity is the velocity of any fixed point of shape factor, *e.g.*, maximum. The difference of group velocities $\Delta v = \Delta v(E, V, \theta, \Delta m^2)$ does not depend on the oscillation phase. The velocities are constant and do not change in the course of propagation.

If density changes along the neutrino trajectory, v_i^{eff} and Δv^{eff} do depend on distance. In the adiabatic periodically varying density v_i^{eff} can be introduced as the velocities averaged over period:

$$v_i^{eff} = L^{-1} \int_0^L dx \frac{dH_i}{dE} \Big|_{\bar{E}}.$$

Then the condition of infinite coherence is

$$\Delta v^{eff} = L^{-1} \int_0^L dx \frac{d\Delta H}{dE} \Big|_{\bar{E}} = 0.$$

It corresponds to a situation when $\Delta v^{eff}(x) > 0$ in one part of the period and $\Delta v^{eff}(x) < 0$ in another part (23).

The situation is much more complicated if adiabaticity is broken as in the case of a single jump between two layers, discussed in sect. 3. In the second layer, the WP has two components, and it is non-trivial to identify the point of the WP to which the group velocity should

be ascribed. Furthermore, just after crossing the jump, certain parts of the WP will have opposite phases and therefore interfere destructively, so that the interference is the same as before crossing. This also affects shape factors (47) and (48). In this case, the infinite coherence has no meaning apart from specific cases which are reduced to infinite coherence in a single layer (sect. 3).

Infinite coherence (infinite number of periods) has meaning in the castle-wall profile for the (long-range) parametric oscillations. The effective group velocities should be defined for a single period of CW profile similarly to the periodic profile with adiabatic density change considered above. Furthermore, one should take into account (similarly to single jump case) that (80)

- Shape factor of the total WPs changes at the crossings, due to splitting and delays of the components;
- Oscillation phase is different in different parts of the same total WP because of different histories of the elementary components.

As a result, expressions for v_i^{eff} and condition for infinite coherence should depend not only on phases acquired in the layers a and b but also on the mixing in both layers (77).

Indeed we can obtain the condition in the x -representation rewriting condition (56) for $n_{coh} \rightarrow \infty$ in terms of delays t^a and t^b we find:

$$\begin{aligned} [s_a c_b + c_a s_b \cos 2\Delta] t_a + [c_a s_b + s_a c_b \cos 2\Delta] t_b = \\ = s_a s_b \sin 2\Delta \frac{1}{E} \left(\frac{V_a \sin 2\theta_a}{\Delta H_a} - \frac{V_b \sin 2\theta_b}{\Delta H_b} \right), \end{aligned} \quad (87)$$

where we used

$$\frac{d2\theta_m}{dE} = \frac{V_m \sin 2\theta_m}{E \Delta H_m},$$

$m = a, b$. From (87), we see that infinite coherence for parametric oscillations is unrelated to overlaps of the elementary WPs at the end of each period; this is the major difference from the cases where adiabaticity is conserved.

There is no simple interpretation of infinite coherence for parametric oscillations in terms of characteristics of elementary WP. In the Table 1, for three different E_0 , we show the delays of elementary WPs as well as phases and mixings in each layer of the CW profile with parameters (53). No simple correlation is observed.

5 Applications to supernova neutrino evolution

The issues of coherence in matter are of great relevance for oscillations of supernova neutrinos (SN). The reasons are enormous distances from the production points to a detector at the Earth,

E_0 (MeV)	t_a (MeV $^{-1}$)	t_b (MeV $^{-1}$)	ϕ^a (rad)	ϕ^b (rad)	θ_a (rad)	θ_b (rad)
2.3	-0.98	-2.4	1.6	2.7	0.83	0.15
3.3	1.5	-1.2	2.1	1.8	1.3	0.156
7.7	0.4	-0.21	3.87	0.73	1.5	0.2

Table 1: Energies of enhanced coherence length, E_0 , delays, phases and mixing angles in each of the layers a and b of a CW profile with parameters (53).

complicated oscillation and conversion phenomena inside a star, non-trivial profiles of medium potentials. Here we briefly describe some effects, while a detailed study will be presented elsewhere [29].

SN neutrinos are produced at densities $\rho \sim 10^{12}$ g/cm 3 and have very short wave packets $\sigma_x \sim 10^{-11}$ cm [17, 12, 18]. Propagating to the surface of a star they can undergo the collective oscillations at $R < 100$ km [30, 31, 32, 33] and then the resonance flavor conversion at $R > 1000$ km [34, 35, 36, 37, 38, 39]. The collective effects are supposed to be active at certain phases of a neutrino burst [31].

Let us first assume that collective oscillations are absent due to damping effects [40] or due to lack of conditions for these oscillations at certain time intervals. In this case, the standard resonance conversion picture is realized: in the production region, the mixing is strongly suppressed so that the flavor states coincide with the eigenstates of propagation in matter. The coincidence depends on the type of mass hierarchy. Except for special situations (time periods and locations), the adiabaticity condition is well satisfied, and therefore the adiabatic transformations occur when neutrinos travel to the surface: $\nu_i^m \rightarrow \nu_i$ ($i = 1, 2, 3$). The adiabaticity can be broken in fronts of shock waves which affects the described picture.

If the initial fluxes of ν_μ and ν_τ are equal, the results of conversion depend only on the $\nu_e - \nu_e$ survival probability, p , in the neutrino channel and on the $\bar{\nu}_e - \bar{\nu}_e$ probability, \bar{p} , in the antineutrino channel. For definiteness we will consider the $\bar{\nu}_e$ channel. In this case, the flux of $\bar{\nu}_e$ at the surface of the star, and consequently, the Earth equals

$$F_{\bar{\nu}_e} = \bar{p}F_{\bar{\nu}_e}^0 + (1 - \bar{p})F_{\bar{\nu}_x}^0, \quad (88)$$

where $F_{\bar{\nu}_e}^0$ and $F_{\bar{\nu}_x}^0$ are the initial fluxes of $\bar{\nu}_e$ and $\bar{\nu}_x$ (mixture of $\bar{\nu}_\mu$ and $\bar{\nu}_\tau$). The second term in (88) corresponds to transitions $\bar{\nu}_\mu, \bar{\nu}_\tau \rightarrow \bar{\nu}_e$. Derivation of the equation (88) assumes that initially produced ν_i^m (which coincide with the flavor states) are incoherent and evolve independently. Therefore signals produced by ν_i^m or states, to which ν_i^m evolve, sum up incoherently.

For $R \ll 1000$ km, the matter density is much bigger than the density of the H-resonance associated with Δm_{13}^2 . In this matter dominated range, according to Eq. (11) in sect. 2 the coherence length L_{coh}^m is function of the vacuum parameters (see also fig. 1):

$$L_{coh}^m = \frac{L_\nu}{\cos 2\theta} \frac{E}{2\sigma_E} = 1100 \text{ km} \left(\frac{E}{20\text{MeV}} \right) \left(\frac{E}{10\sigma_E} \right).$$

Therefore the WP of eigenstates will separate before reaching the H-resonance even if they overlapped at the production. Notice that with an increase on E , the length L_{coh}^m increases, but the resonance shifts to outer layers. Still, some partial coherence may exist.

For definiteness we assume the inverted mass hierarchy. Then according to the level crossing scheme at the production $\bar{\nu}_3^m \approx \bar{\nu}_e$, $\bar{\nu}_1^m \approx \bar{\nu}_x$ and $\bar{\nu}_2^m = \bar{\nu}_x'$. Furthermore, antineutrinos cross only H-resonance. The dynamics is related to $\bar{\nu}_3^m - \bar{\nu}_1^m$ subsystem, while $\bar{\nu}_2^m$ essentially decouples appearing as a spectator. Therefore the $\bar{\nu}_e$ survival probability can be written as

$$\bar{p} = |U_{e1}|^2 P_{31} + s_{13}^2 (1 - P_{31}),$$

where $P_{31} \equiv P(\bar{\nu}_3^m \rightarrow \bar{\nu}_1^m)$ is the $\bar{\nu}_3^m \rightarrow \bar{\nu}_1^m$ transition probability.

Let us consider the effects of the coherence loss and coherence enhancement under different circumstances.

1. In the completely adiabatic case, $\bar{\nu}_3^m (\approx \bar{\nu}_e)$ evolves to $\bar{\nu}_3$, so that $P(\bar{\nu}_3^m \rightarrow \bar{\nu}_1^m) = 0$ and $\bar{p} = |U_{e3}|^2 = s_{13}^2$. In central parts of a star $\bar{\nu}_1^m$ has larger group velocity than $\bar{\nu}_3^m$. Below the H-resonance, inversely, $\bar{\nu}_3^m$ moves faster and $\bar{\nu}_3$ will arrive at the Earth first.

2. Adiabaticity is strongly broken in a shock wave front which can be considered as the instantaneous density jump (see sect. 3). We will assume that before the jump (layer a) and after the jump (layer b) neutrinos propagate adiabatically. Crossing the jump the eigenstates $\bar{\nu}_1^a$ and $\bar{\nu}_3^a$ split into eigenstates $\bar{\nu}_j^b$. To find \bar{p} we consider evolution of $\bar{\nu}_3^a$ which becomes $c_\Delta \bar{\nu}_3^b - s_\Delta \bar{\nu}_1^b$ after crossing the jump. Then its components $\bar{\nu}_j^b$ loose coherence and evolve to $\bar{\nu}_j$ at the surface of a star. Consequently, we find

$$\bar{p} = c_\Delta^2 s_{13}^2 + s_\Delta^2 |U_{e1}|^2.$$

Strong adiabaticity violation effect on \bar{p} is realized if the change of mixing in matter, Δ , is large. The latter occurs when the jump appears in the resonance layer, and the size of the jump is larger than the width of the resonance layer: $\Delta\rho > \rho_R \tan 2\theta_{13} = 0.3\rho_R$. That is, even a small jump can produce a strong effect.

As we discussed before, the jump regenerates oscillations, which then disappear, and \bar{p} does not depend on the oscillation phase. Single shock front (jump) could lead to phase (coherence) effect, if $\bar{\nu}_1^a$ and $\bar{\nu}_3^a$ are produced in a coherent state (*e.g.*, as a result of collective oscillations) and coherence is supported till the jump. In this case, the result of evolution depends on the phase ϕ^a acquired in the layer a , and this phase is observable. Notice that formula (88) is invalid in this case.

3. Let us consider the case of two density jumps that appear due to the presence of two shock wavefronts: the direct and reversed one. This situation is analogous to the one described in sect. 3. We denote by a , b and g the layers between the production point and the inner (reversed) shock, between two shocks and outside the outer shock correspondingly. The potential of the layer b , V_b can be constant or change adiabatically, the potentials just before inner shock, V_a , and after second shock (jump), V_g , are not equal (in contrast to CW).

The picture of evolution of $\bar{\nu}_3^m$ state is the following:

- $\bar{\nu}_{3m}$ propagates adiabatically in the layer a and splits at the border between a and b :
 $\bar{\nu}_3^a = c_\Delta \bar{\nu}_3^b - s_\Delta \bar{\nu}_1^b$;
- the latter state is coherent and oscillates in the layer b acquiring the oscillation phase ϕ^b :
 $c_\Delta e^{i\phi^b} \bar{\nu}_3^b - s_\Delta \bar{\nu}_1^b$;
- the eigenstates $\bar{\nu}_3^b, \bar{\nu}_1^b$ split in the second jump (the border between b and g): $\bar{\nu}_3^b = c_{\Delta'} \bar{\nu}_3^g - s_{\Delta'} \bar{\nu}_1^g, \bar{\nu}_1^b = c_{\Delta'} \bar{\nu}_1^g + s_{\Delta'} \bar{\nu}_3^g$, where $\Delta' \equiv \theta_g - \theta_b$ is the change of the mixing angle in the second jump;
- in the layer g the eigenstates $\bar{\nu}_j^g$ evolve adiabatically to the mass eigenstates $\bar{\nu}_j^g \rightarrow \bar{\nu}_j$. Furthermore, $\bar{\nu}_1$ and $\bar{\nu}_3$ separate and decohere.

According to this picture we obtain the following expression for the probability \bar{p} :

$$\bar{p} = |U_{e1}|^2 \sin^2(\Delta + \Delta') + s_{13}^2 \cos^2(\Delta + \Delta') - (|U_{e1}|^2 - s_{13}^2) \sin 2\Delta \sin 2\Delta' \sin^2 \frac{\phi^b}{2}. \quad (89)$$

Notice that $\Delta + \Delta' = \theta_g - \theta_a$.

In fig. 4 we plot \bar{p} computed with Eq. (89) for the following values of parameters: $V_a = 6.3 \times 10^{-12}$ eV, $V_b = 3.2 \times 10^{-11}$ eV, $V_g = 3.2 \times 10^{-12}$ eV and $L_b = 1060$ km. If we assume electron fraction $Y_e = 0.5$, the corresponding densities are $\rho_a = 2 \times 10^2$ g/cm³, $\rho_b = 10^3$ g/cm³, $\rho_g = 10^2$ g/cm³. Since the distance between the two shock fronts is much larger than the oscillation length in matter, $l_m < 100$ km, one can naively average the oscillatory terms in (89), *i.e.* take $\sin^2 \phi^b / 2 = 0.5$ (the red curve in fig. 4). However, according to our analysis in sect. 2 in layers of constant and slowly varying densities, the energy range of enhanced coherence exists around E_0 , where oscillation effects might not be negligible. This is shown in fig. 4 by the black curve for the energy resolution $\sigma_E/E = 0.1$. Here $E_0 = 41$ MeV. This oscillation effect will survive further propagation to the Earth, the effect encodes information about distance between shock wave fronts and density profile. Similar effects of enhanced coherence also survives for adiabatic propagation between the two shocks according to (26). As the distance between the two jumps increases, one needs better energy resolution, $\sigma_E/E < 0.1$, to observe the effect of enhanced coherence.

Let us consider the possible effect of the coherence loss on the collective oscillations in central parts of a star. These oscillations are induced by coherent flavor exchange in the $\nu - \nu$ scattering, and high neutrino densities at $r < 100$ km make them relevant.

The critical issue is whether fast loss of coherence due to very short WPss destroys collective oscillations. Indeed, the latter imply the $\nu - \nu$ interactions after neutrino production, which can be considered as ν -detection ("observation") process. Loss of coherence between production and interaction as well as between different interactions can be important. Furthermore, effectively the problem becomes non-linear, and therefore, it is not clear if integration over energies that form the WP can be interchanged with evolution. Such an interchange is in the basis

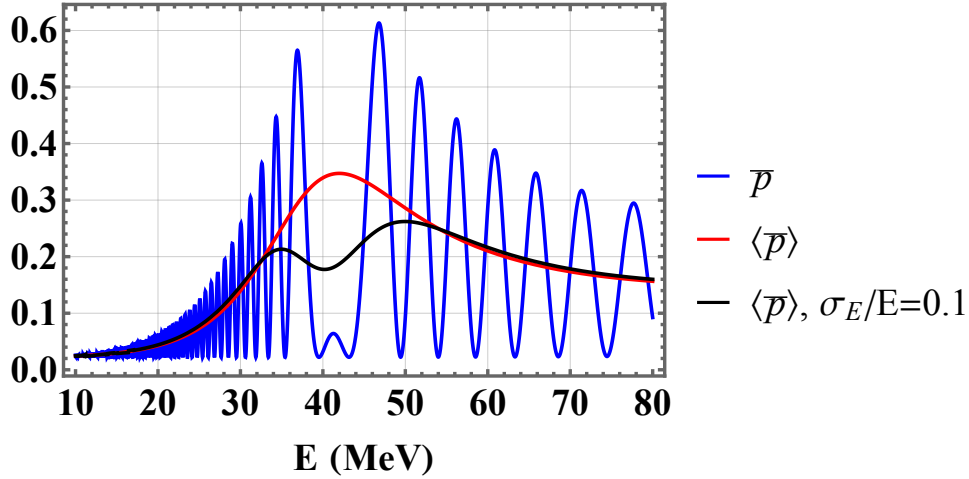


Figure 4: Dependence of the $\bar{\nu}_e$ survival probability in supernova on neutrino energy (blue line). Inverted mass hierarchy and 1-3 vacuum mixing were assumed. The probability averaged over the energy interval $\sigma_E = 0.1E$ is shown by black line. The red line shows the probability without oscillatory term.

of equivalence of results in the x - and E -representations [26]. There is no clear answer to this question [17, 12, 41, 18].

Some new insight into the problem can be obtained using description of the collective oscillations as evolution of the individual neutrinos propagating in effective external potentials formed by matter and background neutrinos [19]. In this case, the problem becomes explicitly linear. Since the background neutrinos oscillate, the effective potentials have non-trivial oscillatory dependence in time (distance). These variations of the potentials are non-adiabatic and therefore strong flavor transitions can be interpreted as parametric oscillations and parametric enhancement effects. Taking into consideration this picture one can apply the results of sect. 4.

The following comments are in order:

1. Propagation decoherence is related to the energy dependence of the Hamiltonian (and consequently the phases). The collective (fast) transformations are driven mainly by potentials that dominate over the vacuum term $\Delta m^2/2E$ (the source of E dependence). The vacuum term (with mixing) triggers conversion at the initial short phase. Therefore, apart from the initial phase, decoherence is simply absent. If the initial phase is short enough the decoherence is entirely irrelevant.

2. In the region of fast collective oscillations, $r_{coll} < 100$ km, with strong matter dominance the coherence length is given by vacuum parameters (89) and turns out to be $L_{coh} \sim 10^3$ km. So, $r_{coll} \ll L_{coh}$ and decoherence can be neglected for $r < r_{coll}$.

3. For low energies ($E \sim 10$ MeV) and $\sigma_E \sim E$ the length $L_{coh} < 10^2$ km can be comparable to the scale of collective oscillations. However, this estimation of L_{coh} is for constant density. As we established in sect. 4, the parametric oscillations themselves can substantially

enhance coherence at least in certain energy intervals around E_0 . So, here we deal with coherence sustained by oscillatory dependence of potentials.

Notice that consideration of coherence for collective oscillations was problematic because of strong adiabaticity violation and difficulty to define the eigenstates. Using analogy with the CW case, this can be done by integrating the Hamiltonian over one period, thus eliminating fast variations. For the averaged Hamiltonian, one can introduce the eigenstates and their effective group velocities. Then the enhanced coherence corresponds to approximate equality of these group velocities (87).

6 Conclusions

The propagation decoherence occurs due to the difference of the group velocities, which leads to the shift of the WPs relative to each other and their eventual separation. In matter, due to refraction, both the group and phase velocities of neutrinos change with respect to the vacuum velocities. Thus, the refraction affects the propagation coherence (and decoherence).

The consideration of WPs in the x -space with average energy and momentum produces the same results as consideration of plane waves in the E -space and integration of probability (oscillation phase) over the energy spectrum with width given by the energy uncertainty. In particular, the same value of the coherence length follows from both approaches.

For different density profiles, we determined the coherence lengths and their dependence on neutrino energy. The salient feature in matter is the existence of infinite coherence length, $L_{coh} \rightarrow \infty$, at certain energies E_0 , and regions of enhanced coherence around E_0 . In the energy space, E_0 is given by zero derivatives of the phase on energy. In the configuration space, it follows from equality of the group velocities of the eigenstates. The condition can be described as the energy of minimal averaging of the interference term of the probability.

The fundamental notion here is the effective group velocities which depend on the density profiles.

1. For constant density the infinite coherence $E_0 = E_R / \cos 2\theta$ coincides with the MSW resonance energy in oscillations of mass eigenstates $\nu_1 \leftrightarrow \nu_2$, and for small vacuum mixing, it is close to the MSW flavor resonance. The width of the region of enhanced coherence (weak averaging) is inversely proportional to the energy resolution, σ_E , and grows according to $\propto E_0^2$. For very large densities (high energies), the coherence length is determined by vacuum parameters and becomes close to the coherence length in vacuum: $L_{coh}^m = L_{coh} / \cos 2\theta$.

For massless neutrinos and oscillations driven by matter the coherence is supported infinitely for all the energies.

2. In varying density profiles, the infinite coherence is realized in particular situations. For monotonously and adiabatically changing density the coherence length can increase toward specific energy E_0 , which corresponds to certain V_0 , such that for $V > V_0$ and $V < V_0$ separation have opposite signs and compensate each other.

Infinite coherence can be realized for periodic profile with adiabatic density change. It

corresponds to equality of the group velocities of eigenstates averaged over the period. E_0 can be found from the latter condition.

3. In the presence of adiabaticity violation, transitions between eigenstates of propagation happen. This leads to modification of WP shape, and consequently, to change of the effective group velocities.

We considered in details the case of maximal adiabaticity breaking - density jumps in certain points of space (neutrino trajectory). In this case, two new effects are realized, which are related to the split of the eigenstates at borders between layers: (i) spread of total WP, (ii) change of the oscillation phase along these total WPs.

For the example of a single jump between two layers with different constant densities, there are two components in the first layer and four components in the second. Correspondingly there are various group velocities and oscillation phases at a detector, and it is not possible to introduce the coherence length in the usual way. Still the medium parameters can be selected so that some level of coherence can be supported for long distances because the split of the eigenstates regenerates interference and oscillations.

4. We checked that modifications of the total WP in the x -space do not change its Fourier transform to the E -space, and consequently, the energy spectrum of neutrinos. Therefore derivation of the infinite coherence conditions for complicated density profiles can be more accessible in the E -representation.

In certain situations, consideration of WP in the x -space simplifies computations of probabilities, especially when coherence is completely lost. Moreover, it becomes crucial when time tagging is introduced at the production or detection, breaking the stationarity condition.

5. For periodic structures with density jumps, such as the castle-wall profile, the coherence length can be introduced for the parametric oscillations (and not for small scale coherence of elementary WP). Then the coherence can be supported for many periods. For parametric oscillations, there are several E_0 , each associated with a particular parametric resonance.

Interpretation of the condition for E_0 in x -space in terms of elementary WPs propagating in the individual layers of the profile is very non-trivial. We find that the effective group velocities for one period (and therefore the infinite coherence condition) are rather complicated functions of mixing angles, phases and delays acquired by the elementary WPs in two parts of the period.

6. Using elementary WPs, we reconstructed total WPs at a detector and studied their spread and shape change in the course of propagation depending on parameters of the CW profile. The reconstruction of the total WP from the elementary WP using operators of time shift is presented. Resummation of the elementary WP at a detector can be performed using the evolution matrix for one period expressed in terms of operators of time shifts.

7. We outlined applications of the obtained results to supernova neutrinos. In particular, we showed that coherence can be supported between two shock wavefronts, leading to observable oscillation effects at the Earth.

For collective oscillations due to large matter potentials the coherence is determined by vacuum parameters and coherence length is much larger than the scale of fast oscillations. Using interpretation of collective oscillations as the parametric effects we find that coherence

can be further enhanced in certain energy ranges.

7 Acknowledgements

YPPS acknowledges support from FAPESP funding Grants No. 2014/19164-453 6, No. 2017/05515-0 and No. 2019/22961-9.

References

- [1] Boris Kayser. On the Quantum Mechanics of Neutrino Oscillation. Phys. Rev., D24:110, 1981.
- [2] Ken Kiess, Shmuel Nussinov, and Nathan Weiss. Coherence effects in neutrino oscillations. Phys. Rev., D53:537–547, 1996.
- [3] C. Giunti and C. W. Kim. Coherence of neutrino oscillations in the wave packet approach. Phys. Rev., D58:017301, 1998.
- [4] W. Grimus, P. Stockinger, and S. Mohanty. The Field theoretical approach to coherence in neutrino oscillations. Phys. Rev. D, 59:013011, 1999.
- [5] C. Giunti. Neutrino wave packets in quantum field theory. JHEP, 11:017, 2002.
- [6] Evgeny Kh. Akhmedov and Alexei Yu. Smirnov. Paradoxes of neutrino oscillations. Phys. Atom. Nucl., 72:1363–1381, 2009.
- [7] Evgeny Kh. Akhmedov and Joachim Kopp. Neutrino Oscillations: Quantum Mechanics vs. Quantum Field Theory. JHEP, 04:008, 2010. [Erratum: JHEP10,052(2013)].
- [8] Evgeny Akhmedov, Daniel Hernandez, and Alexei Smirnov. Neutrino production coherence and oscillation experiments. JHEP, 04:052, 2012.
- [9] Evgeny Akhmedov. Quantum mechanics aspects and subtleties of neutrino oscillations. In International Conference on History of the Neutrino: 1930-2018 Paris, France, September 5-7, 2018, 2019.
- [10] S. P. Mikheev and A. Yu. Smirnov. Resonant amplification of neutrino oscillations in matter and solar neutrino spectroscopy. Nuovo Cim. C, 9:17–26, 1986.
- [11] S. P. Mikheev and A. Yu. Smirnov. Neutrino Oscillations in an Inhomogeneous Medium: Adiabatic Regime. Sov. Phys. JETP, 65:230–236, 1987.
- [12] Joern Kersten and Alexei Yu. Smirnov. Decoherence and oscillations of supernova neutrinos. Eur. Phys. J., C76(6):339, 2016.

- [13] F. Benatti and R. Floreanini. Open system approach to neutrino oscillations. JHEP, 02:032, 2000.
- [14] S. P. Mikheyev and A. Yu. Smirnov. Resonant neutrino oscillations in matter. Prog. Part. Nucl. Phys., 23:41–136, 1989.
- [15] Hajime Anada and Haruhiko Nishimura. Coherence condition for resonant neutrino oscillation. Phys. Rev. D, 41:2379–2383, Apr 1990.
- [16] J. T. Peltoniemi and V. Sipilainen. Neutrino propagation in matter using the wave packet approach. JHEP, 06:011, 2000.
- [17] Jörn Kersten. Coherence of Supernova Neutrinos. Nucl. Phys. B Proc. Suppl., 237-238:342–344, 2013.
- [18] Evgeny Akhmedov, Joachim Kopp, and Manfred Lindner. Collective neutrino oscillations and neutrino wave packets. JCAP, 09:017, 2017.
- [19] Rasmus S.L. Hansen and Alexei Yu Smirnov. Neutrino conversion in a neutrino flux: Towards an effective theory of collective oscillations. JCAP, 04:057, 2018.
- [20] Rasmus S.L. Hansen and Alexei Yu Smirnov. Effect of extended ν production region on collective oscillations in supernovae. JCAP, 10:027, 2019.
- [21] Evgeny K. Akhmedov. Neutrino oscillations in inhomogeneous matter. (In Russian). Sov. J. Nucl. Phys., 47:301–302, 1988.
- [22] P. I. Krastev and A. Yu. Smirnov. Parametric Effects in Neutrino Oscillations. Phys. Lett. B, 226:341–346, 1989.
- [23] Evgeny K. Akhmedov. Parametric resonance of neutrino oscillations and passage of solar and atmospheric neutrinos through the earth. Nucl. Phys. B, 538:25–51, 1999.
- [24] Evgeny K. Akhmedov. Parametric resonance in neutrino oscillations in matter. Pramana, 54:47–63, 2000.
- [25] Evgeny K. Akhmedov and A.Yu. Smirnov. Comment on ‘New conditions for a total neutrino conversion in a medium’. Phys. Rev. Lett., 85:3978, 2000.
- [26] Leo Stodolsky. The Unnecessary wave packet. Phys. Rev. D, 58:036006, 1998.
- [27] Sebastian Hollenberg and Heinrich Pas. Adiabatic & non-adiabatic perturbation theory for coherence vector description of neutrino oscillations. Phys. Rev. D, 85:013013, 2012.
- [28] L. Wolfenstein. Neutrino Oscillations in Matter. Phys. Rev. D, 17:2369–2374, 1978.

- [29] Y. P.P. Silva and A. Y. Smirnov. Work in progress.
- [30] Huaiyu Duan, George M. Fuller, and Yong-Zhong Qian. Collective Neutrino Oscillations. Ann. Rev. Nucl. Part. Sci., 60:569–594, 2010.
- [31] Alessandro Mirizzi, Irene Tamborra, Hans-Thomas Janka, Ninetta Saviano, Kate Scholberg, Robert Bollig, Lorenz Hudepohl, and Sovan Chakraborty. Supernova Neutrinos: Production, Oscillations and Detection. Riv. Nuovo Cim., 39(1-2):1–112, 2016.
- [32] Sovan Chakraborty, Rasmus Sloth Hansen, Ignacio Izaguirre, and Georg Raffelt. Self-induced neutrino flavor conversion without flavor mixing. JCAP, 03:042, 2016.
- [33] Irene Tamborra and Shashank Shalgar. New Developments in Flavor Evolution of a Dense Neutrino Gas. 11 2020.
- [34] L. Wolfenstein. Neutrino Oscillations and Stellar Collapse. Phys. Rev. D, 20:2634–2635, 1979.
- [35] S. P. Mikheev and A. Yu. Smirnov. Neutrino Oscillations in a Variable Density Medium and Neutrino Bursts Due to the Gravitational Collapse of Stars. Sov. Phys. JETP, 64:4–7, 1986.
- [36] Amol S. Dighe and Alexei Yu. Smirnov. Identifying the neutrino mass spectrum from the neutrino burst from a supernova. Phys. Rev. D, 62:033007, 2000.
- [37] Cecilia Lunardini and Alexei Yu. Smirnov. Probing the neutrino mass hierarchy and the 13 mixing with supernovae. JCAP, 06:009, 2003.
- [38] R. Tomas, Michael Kachelriess, G. Raffelt, A. Dighe, H. T. Janka, and L. Scheck. Neutrino signatures of supernova shock and reverse shock propagation. JCAP, 09:015, 2004.
- [39] Basudeb Dasgupta and Amol Dighe. Phase effects in neutrino conversions during a supernova shock wave. Phys. Rev. D, 75:093002, 2007.
- [40] Georg G. Raffelt and Irene Tamborra. Synchronization versus decoherence of neutrino oscillations at intermediate densities. Phys. Rev. D, 82:125004, 2010.
- [41] Evgeny Akhmedov and Alessandro Mirizzi. Another look at synchronized neutrino oscillations. Nucl. Phys. B, 908:382–407, 2016.